

Enhanced Performance with Bismuth Ferrite Perovskite in ZnO Nanorod Solid State Solar Cells

Supporting Information

Leonard Loh, Joe Briscoe* and Steve Dunn

Corresponding Author Email: j.briscoe@qmul.ac.uk

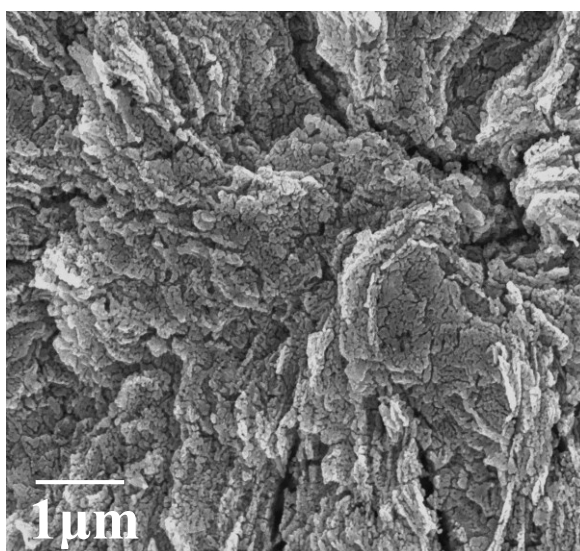


Figure S1. Dissolution of ZnO with BFO sol

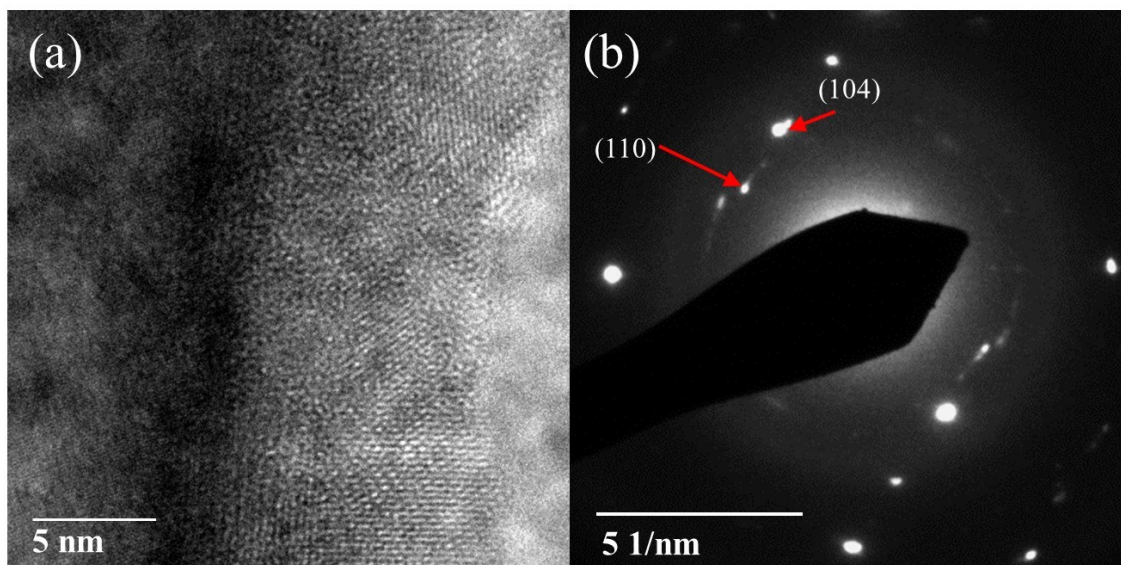


Figure S2. (a) HRTEM image of conformally coated BFO ZnO nanorods. The BFO coating shows well crystallized film with minimal amorphous structure detected. The presence of several crystal planes also indicate polycrystalline coatings (b) SAED pattern of BFO coating shows presence of (104) and (110) crystal planes.

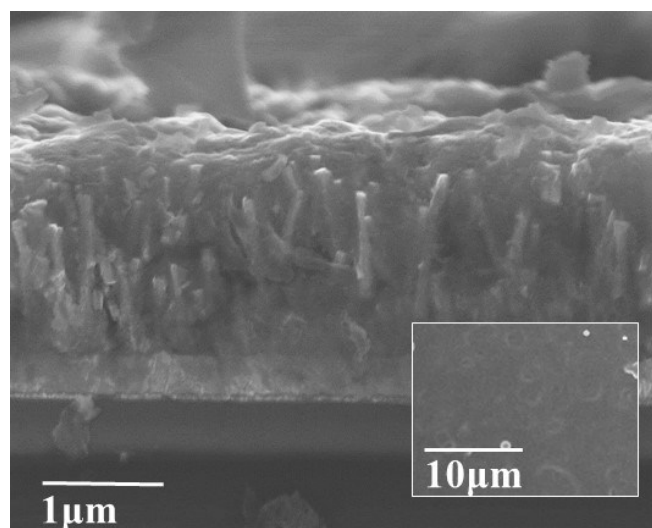


Figure S3. Cross sectional view of CuSCN infiltrated ZnO/BFO nanorods structure (inset shows topographical view)

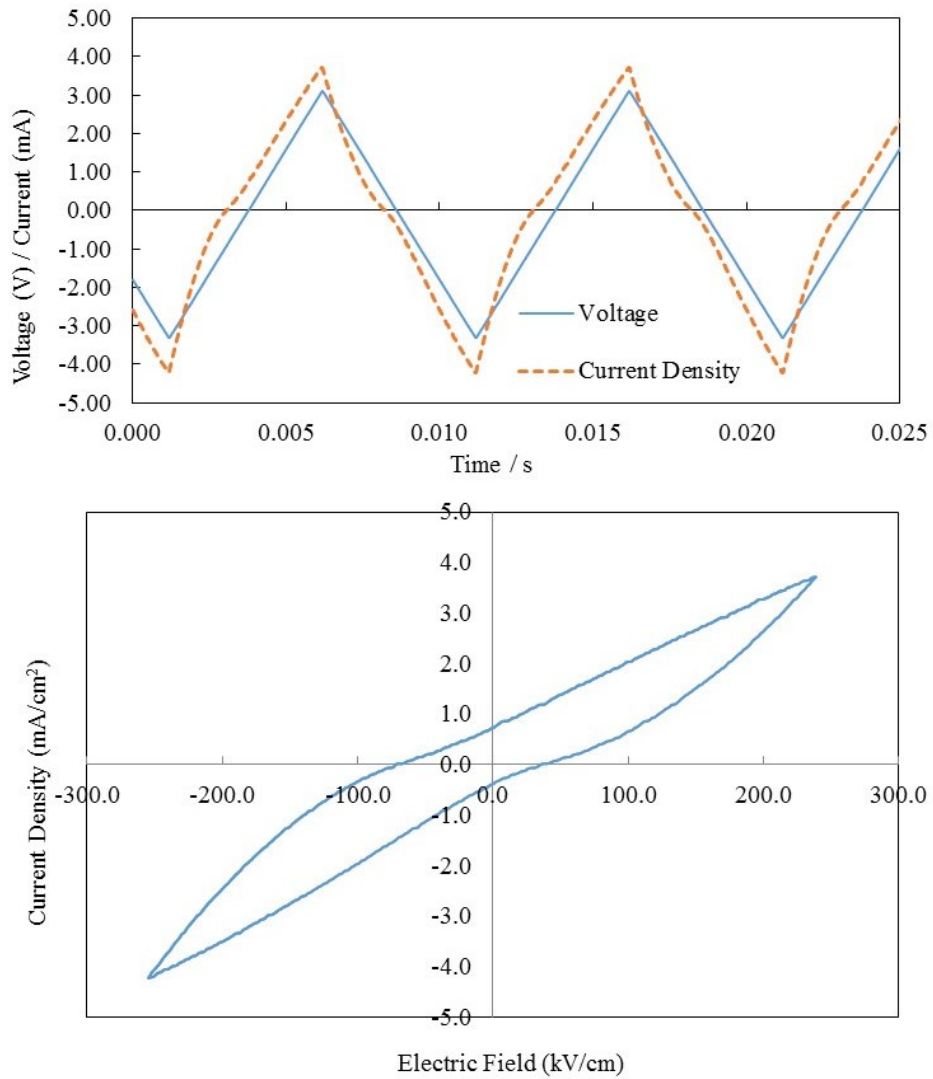


Figure S4. Ferroelectric measurements of 520 nm thick BFO film with 3.25 V charging amplitude and 100 Hz frequency (a) Voltage and current output in the time domain (b) Electric field - Current density curves for the devices

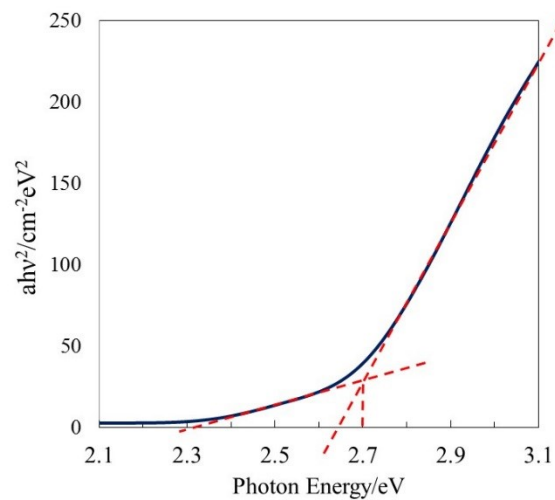


Figure S5. Tauc plot for BFO thin film

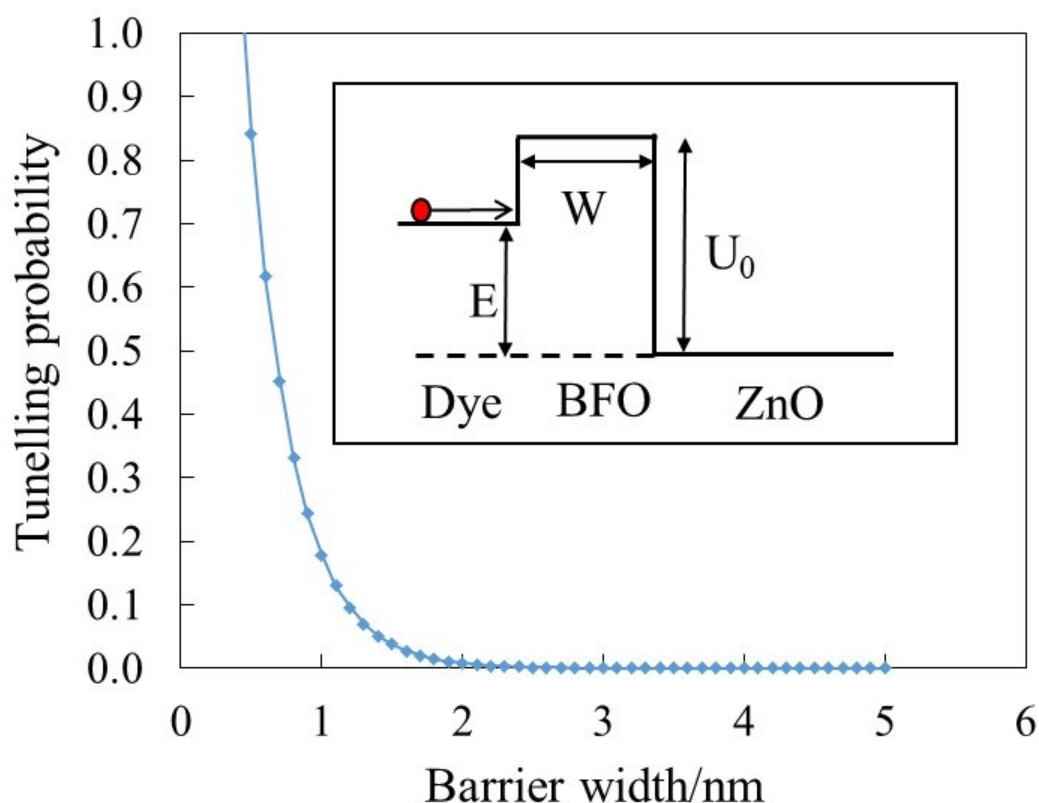


Figure S6. Probability of an electron tunnelling from the N719 dye to ZnO through a BFO layer of width W , where E is the energy of the LUMO of the N719 dye, and U_0 is the difference between the conduction band potentials of ZnO and BFO as shown in the inset schematic. This was calculated assuming a rectangular barrier based on the tunnelling probability:

$$P \approx \frac{16E(U_0 - E)}{U_0^2} \exp\left(-2\sqrt{\frac{2m^*(U_0 - E)}{\hbar^2}}W\right)$$

(S.M. Sze, *Physics of Semiconductor Devices*, Wiley 2007) and an electron effective mass of $0.2m_e$ (P. Pipinys, A. Rimeika, V. Lapeika, *Ferroelectrics* **2010**, 396, 60). This will tend to underestimate the tunnelling probability as it omits the in-built field between the BFO and ZnO which creates a more field-emission-type system with a driving force for electron transfer. However the exact nature of this field is not known and therefore cannot be included in the calculation.